10.1109/ULTSYM.2014.0155

Effective scatterer size estimates in HT-29 spheroids at 55 MHz and 80 MHz

L.A. Wirtzfeld[1], E.S.L. Berndl[1], G.J. Czarnota[2] and M.C. Kolios[1]

[1]Department of Physics
Ryerson University
Toronto, Canada
mkolios@ryerson.ca

[2]Department of Radiation Oncology and Imaging
Sunnybrook Health Sciences Centre
Toronto, Ontario, Canada

***Abstract*— Spheroids provide a three-dimensional in-vitro model of cell-to-cell interaction and basic structure. High-frequency ultrasound studies of spheroids show good image contrast between viable rims and necrotic cores, but spectral analyses have not been performed. This study examines colorectal HT-29 spheroids using high-frequency ultrasound at 55MHz (n=5) and 80MHz (n=4) to determine changes in spectral parameters as a function of transducer frequency and location (core vs rim). Histology shows low cell density within the core and a tightly packed rim, which forms a smooth shell. Statistically significant differences were found in the midband fit, spectral slope and effective scatterer diameter estimate as a function of imaging frequency and spheroid location. Effective scatterer diameter estimates (12.7 ± 0.4 µm at 55MHz and 6.6 ± 0.5 µm at 80MHz) agree closely with histological estimates (12.9 ± 0.3 µm for the cell and 7.0 ± 0.3 µm for the nucleus) suggesting different primary scatterers at the two frequencies.**

Keywords—high-frequency ultrasound, quantitative ultrasound, HT-29 spheroids

I. Introduction

The use of spectral and quantitative techniques in ultrasound, rather than qualitative images based on the log-compressed RF data, allows subtle differences in cellular and tissue architecture to be probed. In cancer imaging, quantitative ultrasound has been used to differentiate benign versus malignant tumors [1], different types of malignant tumors [2] and individual cells and tissues undergoing apoptosis [3].

Models that allow the three-dimensional organization of cellular structure to be examined are required in order to develop an understanding of how spectral and quantitative ultrasound parameters are influenced by structural features and changes in these features. Studies have been conducted with individual cells [3], pellets of spun cells [4, 5] and cells in 3D scaffolds [6, 7], which allow for an in-vitro examination of cells. However, the lack of biologically relevant organization and communication limits the ability to draw inferences applicable to in-vivo cellular structure and organization. In-vivo models introduce the complexities of the vasculature and have increased biological variability, which makes determining the contributions of different components to the ultrasound backscatter difficult. A model that better spans the gap between individual cells and an in-vivo model are spheroids where the cells spontaneously form a three-dimensional structure. Spheroids are a well-established model which has been used as a 3D in-vitro model [8-10] for a wide range of studies.

Spheroids were used in one of the first demonstrations of the use of high-frequency (20-100 MHz) ultrasound imaging [10]. In these experiments, there was rich contrast between the viable rim and necrotic core in C-mode images. Quantitative methods have not previously been applied to spheroids to observe changes between the rim and core. The study presented here uses high-frequency ultrasound to evaluate changes in quantitative ultrasound parameters in spheroids due to heterogeneity in cellular growth and as a function of transducer frequency.

II. Material and Methods

A. Spheroids

HT-29 human colorectal adenocarcinoma cells, (ATCC, Manassas, VA) were grown in McCoy's 5a medium (Gibco, NY; prepared at Princess Margaret Hospital, Toronto), supplemented with 10% fetal bovine serum (Gibco, NY) at 37°C at 5% CO_2 in a humidified incubator. Cells were passed at 60-80% confluence to maintain exponential growth. HT-29 spheroids were produced by the hanging drop method [11], seeding each 20 µL drop with 5000 cells for 96 hours at 37°C, 5% CO_2.

B. Ultrasound Imaging

Spheroids were imaged in a large polystyrene plate with a VisualSonics Vevo770 (Toronto, ON) using a nominal 55 MHz single element transducer digitized at 420 MHz and a SASAM acoustic microscope (Kibero GmbH, Germany) using an 80 MHz transducer digitized at 1 GHz. Several imaging planes with the associated digital RF data were acquired through each spheroid ensuring the reflection from the plate region proximal to the spheroid was obtained as a reference for data processing.

C. Histology and Cell Size Estimation

To prepare for histological processing, spheroids were suspended in Tissue Tek optimal cutting temperature medium (Sakura USA, Torrence, CA), and flash frozen in liquid nitrogen. The frozen samples were stored in a -85°C freezer for up to 1 week before processing. Frozen sections were cut to 6 µm slices using a Leica cryostat, and then stained

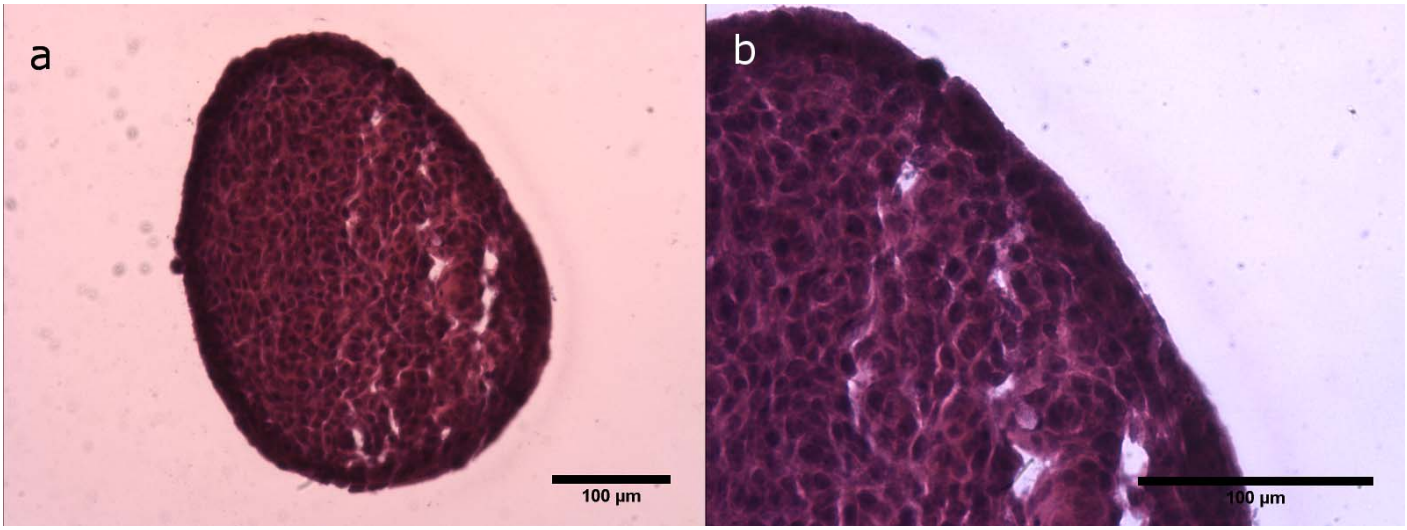

Fig. 1. Histological cross section of a spheroid shown at, (a) 10x and (b) 20x. To prepare the histology samples, the spheroids were flash frozen and stained for H&E. A darker, more compact rim is seen around the edge of the spheroid.

with H&E (Hematoxolin and Eosin). Cell and nucleus diameters were estimated for the rim and core of each initial seeding density by randomly selecting 20 cells per histology slide, which were manually outlined in ImageJ [12]; the reported area was used to calculate an estimated diameter assuming a perfect circle.

D. Data Processing

1) Segmentation

Data from the spheroids were divided into five by five wavelength analysis windows with 75% overlap for data processing. To determine the overall region of interest to process, manual segmentation was performed. First the entire spheroid was outlined and then, when visible on the B-mode image, the central core was outlined. Analysis windows in which at least 75% of the pixels were contained within the segmented central region were considered part of the core of the spheroid. All the other analysis windows were considered part of the rim. The small size of the spheroids limited the analysis window size possible to ensure the two regions could be separately outlined and to avoid substantial overlap with the background.

2) Attenuation

In order to compensate for attenuation, a linear attenuation coefficient estimated by an insertion loss technique from the preceding spheroid experiment was used. A value of 1.4 dB/cm/MHz was used for attenuation correction for all spheroids.

3) Spectral Parameters and Effective Scatterer Diameter

Based on the approach developed by Lizzi et al [13], a linear regression was performed on the normalized, attenuation compensated power spectra for each analysis window, over the bandwidth of the respective transducer. The midband fit (magnitude of the fitted line at the centre of the bandwidth) and spectral slope were computed from the linear regression to allow for comparison across samples.

From the attenuation compensated and normalized power spectra, the backscatter coefficient (BSC) was calculated according to the method proposed by Chen et al. [14]. The Effective Scatterer Diameter (ESD) was estimated based on the fluid filled sphere form factor from [15]. Radii over the range of 0.1 µm to 1 µm (in 0.1 µm steps) and 1 µm to 50 µm (in 1 µm steps) were compared to the estimated BSC. The radius resulting in the lowest mean square error between the theoretical and estimated BSC was selected. Parametric images of the ESD were plotted to allow for any spatial variations in the estimates to be observed.

E. Statistical Analysis

N-way ANOVAs were performed in Matlab to determine if there were statistically significant differences in parameters estimates for the variables of transducer frequency, number of cells seeded or the rim versus core. For cases of a statistically significant result from the ANOVA, post hoc Tukey-Kramer tests were performed.

III. RESULTS

Five spheroids were imaged at 55 MHz and four spheroids were imaged at 80 MHz. Average estimates for the rim and core for each spheroid were calculated by averaging across all analysis windows.

A. Histology

Fig. 1 shows a histological slice of a spheroid seeded with 5000 cells at 10x and 20x magnification. The density of cells varies radially with a less dense core and tightly packed rim. Estimates of size from the histological slices were 12.9 ± 0.3 µm for the cell diameter and 7.0 ± 0.3 µm for the nucleus diameter.

B. Spectral parameters and ESD

ANOVAs indicate significant differences between transducer frequency and location for the spectral slope,

TABLE I. MEANS OF THE MIDBAND FIT, SPECTRAL SLOPE AND EFFECTIVE SCATTERER DIAMETER (ESD) FOR EACH TRANSDUCER FREQUENCY (55 MHZ N=5; 80 MHZ N=4), LOCATION (RIM VS CORE) AND OVERALL.

		Rim	Core	Total
Mean Spectral Slope (dB/MHz)	55MHz	0.17±0.04	0.31±0.04	**0.24±0.03**
	80MHz	0.07±0.04	0.20±0.05	**0.13±0.03**
	Total	**0.11±0.03**	**0.25±0.03**	
Midband Fit (dB)	55MHz	-52.7±0.8	-56.5±0.8	**-54.6±0.6**
	80MHz	-40.0±0.9	-44.1±1.0	**-42.1±0.7**
	Total	**-46.4±0.6**	**-50.3±0.7**	
ESD (µm)	55MHz	13.8±0.6	11.6±0.6	**12.7±0.4**
	80MHz	7.1±0.6	6.1±0.7	**6.6±0.5**
	Total	**10.5±0.4**	**8.9±0.5**	

midband fit and ESD. The average values of these parameters are summarized in Table 1. For both transducers, the spectral slope for the spheroid cores were consistently higher than for the rims. When comparing the measurements from the two transducers, lower average values were obtained at 80 MHz compared to 55 MHz. The midband fit average was lower in the core compared to the rim in both cases. Moreover, the MBF was -54.6 dB at 55 MHz versus -42.1 dB at 80 MHz. ESD core estimates were consistently lower than rim estimates, at both frequencies (by about 1 µm). Averaged estimates of the combined ESD (rim and core) were 12.7 ± 0.4 µm at 55 MHz and 6.6 ± 0.5 µm at 80 MHz.

Fig. 2 and Fig. 3 present representative B-mode and parametric images from the 55 MHz and 80 MHz transducer respectively. The local variations in the spectral slope are seen in Fig. 2b and 3b, with larger values toward the center of the spheroids. Fig. 2c and 3c are parametric images of the midband fit with the lowest values in the same region as the lowest echogenicity in the B-mode images. Fig. 2d and 3d show the ESD values with increased ESD toward the outer edge of the spheroid.

IV. DISCUSSION

The work presented here demonstrates the ability of high-frequency ultrasound to detect subtle variations in structure and organization in even small samples of cells, such as spheroids. The distinct estimates of scatterer size between the two imaging frequencies suggest there could be a change in sensitivity to structures of different sizes.

Estimates of HT-29 cellular size from both the literature and direct measurements of histological slides (approximately 12.9 µm) agree well with the ESD estimates at 55 MHz (average of 12.7 µm), however, the nucleus diameter (approximately 7.0 µm) rather than the cell diameter was much closer to the 80 MHz ESD estimate (average 6.6 µm). The correspondence of these numbers suggests the two frequencies are sensitive to different specific structures within the cells, which opens the possibility of being able to probe changes to the different structures in response to a treatment.

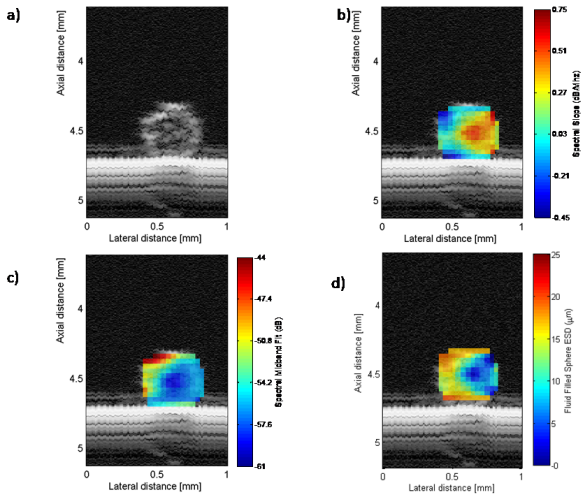

Fig. 2. B-mode (a) image of an example spheroid at 55 MHz. Parametric images overlaid on the Bmode image show the estimated spectral slope (b), midband fit (c) and fluid filled sphere ESD (d). Heterogeneity throughout the spheroid is visible.

The cores, which appeared darker on B-mode images, resulted in a consistent decreased midband fit relative to the brighter rims. Histologically a reduced cellular number density is observed in the cores of the spheroids, reducing the number of scatterers per resolution volume.

V. CONCLUSION

Tumor spheroids allow for the study of a three-dimensional, self-assembled structure to examine the sensitivity of ultrasound to variations within the structure. Variations were observed for all the spectral parameters using RF data collected with a 55 MHz and 80 MHz transducer. Moreover, spectral parameters varied between the core and rim of the spheroids, consistent with the histological results. The ESD estimates in particular showed distinct populations between the two transducers with the 55 MHz estimates and 80

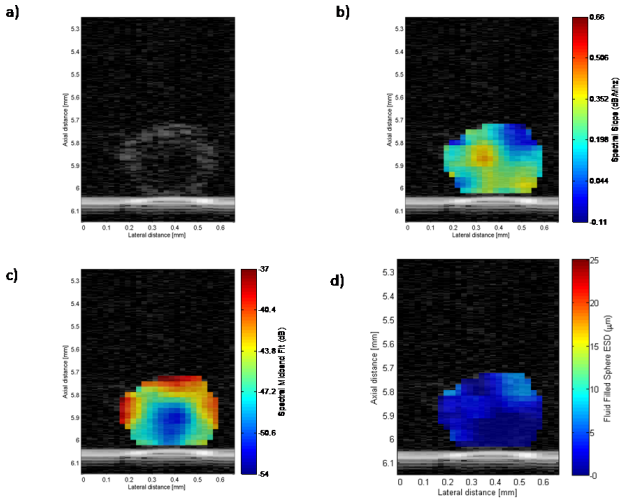

Fig. 3. B-mode (a) image of an example spheroid at 80 MHz. Parametric images overlaid on the Bmode image show the estimated spectral slope (b), midband fit (c) and fluid filled sphere ESD (d). Heterogeneity throughout the spheroid is visible.

MHz estimates agreeing well with histology estimates of cell and nucleus size estimates.

ACKNOWLEDGMENTS

The authors would like to acknowledge funding from a project grant entitled "Imaging for Cancer" from the Terry Fox Foundation (CIHR#TFF 105267) and the Canadian Foundation for Innovation. The authors would also like to acknowledge the Bioacoustic Research Laboratory at the University of Illinois for the shared GUI for BSC computations (NIH grant # CA111289). Travel funds provided by the Candian Cancer Society (grant #703093).

REFERENCES

1. M. L. Oelze, W. D. O'Brien Jr, J. P. Blue, and J. F. Zachary, "Differentiation and characterization of rat mammary fibroadenomas and 4T1 mouse carcinomas using quantitative ultrasound imaging," *IEEE Trans Med Imaging*, vol. 23, no. 6, pp. 764–771, Jun. 2004.
2. M. L. Oelze and W. D. O'Brien, "Application of Three Scattering Models to Characterization of Solid Tumors in Mice," *Ultrason Imaging*, vol. 28, no. 2, pp. 83–96, Apr. 2006.
3. E. Strohm, G. J. Czarnota, and M. C. Kolios, "Quantitative measurements of apoptotic cell properties using acoustic microscopy," *IEEE Trans Ultrason Ferroelectr Freq Control*, vol. 57, no. 10, pp. 2293–2304, Oct. 2010.
4. G. J. Czarnota, M. C. Kolios, H. Vaziri, S. Benchimol, F. P. Ottensmeyer, M. D. Sherar, and J. W. Hunt, "Ultrasonic biomicroscopy of viable, dead and apoptotic cells," *Ultrasound in Medicine & Biology*, vol. 23, no. 6, pp. 961–965, 1997.
5. M. C. Kolios, G. J. Czarnota, M. Lee, J. W. Hunt, and M. D. Sherar, "Ultrasonic spectral parameter characterization of apoptosis," *Ultrasound in Medicine & Biology*, vol. 28, no. 5, pp. 589–597, May 2002.
6. A. Han, R. Abuhabsah, R. J. Miller, S. Sarwate, and W. D. O'Brien Jr, "The measurement of ultrasound backscattering from cell pellet biophantoms and tumors ex vivo," *J. Acoust. Soc. Am.*, vol. 134, no. 1, pp. 686–693, Jul. 2013.
7. K. P. Mercado, M. Helguera, D. C. Hocking, and D. Dalecki, "Estimating Cell Concentration in Three-Dimensional Engineered Tissues Using High Frequency Quantitative Ultrasound," *Ann Biomed Eng*, Mar. 2014.
8. J. P. Freyer and R. M. Sutherland, "Regulation of Growth Saturation and Development of Necrosis in EMT6/Ro Multicellular Spheroids by the Glucose and Oxygen Supply," *Cancer Res*, vol. 46, no. 7, pp. 3504–3512, Jul. 1986.
9. J. Friedrich, W. Eder, J. Castaneda, M. Doss, E. Huber, R. Ebner, and L. A. Kunz-Schughart, "A Reliable Tool to Determine Cell Viability in Complex 3-D Culture: The Acid Phosphatase Assay," *J Biomol Screen*, vol. 12, no. 7, pp. 925–937, Oct. 2007.
10. M. D. Sherar, M. B. Noss, and F. S. Foster, "Ultrasound backscatter microscopy images the internal structure of living tumour spheroids," *Nature*, vol. 330, no. 6147, pp. 493–495, Dec. 1987.
11. D. Del Duca, T. Werbowetski, and R. F. Del Maestro, "Spheroid preparation from hanging drops: characterization of a model of brain tumor invasion," *J. Neurooncol.*, vol. 67, no. 3, pp. 295–303, May 2004.
12. W.S. Rasband, ImageJ, U. S. National Institutes of Health, Bethesda, Maryland, USA, http://imagej.nih.gov/ij/, 1997-2014.
13. F. L. Lizzi, M. Greenebaum, E. J. Feleppa, M. Elbaum, and D. J. Coleman, "Theoretical framework for spectrum analysis in ultrasonic tissue characterization," *J. Acoust. Soc. Am.*, vol. 73, no. 4, pp. 1366–1373, Apr. 1983.
14. X. Chen, D. Phillips, K. Q. Schwarz, J. G. Mottley, and K. J. Parker, "The measurement of backscatter coefficient from a broadband pulse-echo system: a new formulation," *IEEE Transactions on Ultrasonics, Ferroelectrics and Frequency Control*, vol. 44, no. 2, pp. 515–525, Mar. 1997.
15. M. F. Insana, R. F. Wagner, D. G. Brown, and T. J. Hall, "Describing small-scale structure in random media using pulse-echo ultrasound," *J Acoust Soc Am*, vol. 87, no. 1, pp. 179–192, Jan. 1990.
16. Kolios MC, "Biomedical Ultrasound Imaging: from 1 to 1000 MHz" *Canadian Acoustics / Acoustique Canadienne,* vol. 37, no. 3, pp. 35- 42, 2009.